Monte Carlo and density functional theory analysis of the distribution of gold and palladium atoms on Au/Pd(111) alloys

Jorge A. Boscoboinik,[1] Craig Plaisance,[2] Matthew Neurock,[2] and Wilfred T. Tysoe[1,*]
[1]*Department of Chemistry and Biochemistry and Laboratory for Surface Studies, University of Wisconsin-Milwaukee, Milwaukee, Wisconsin 53211, USA*
[2]*Department of Chemical Engineering, University of Virginia, 102 Engineers' Way, Charlottesville, Virginia 22904, USA*
(Received 25 September 2007; published 23 January 2008)

The total energies of various Au/Pd(111) alloys are calculated using density functional theory and the results parametrized by a model that includes the energy to exchange gold and palladium atoms within the first and second layers of the alloy, and between the first and second layers. The model is in excellent agreement with the results of density functional theory calculations giving a net repulsive energy between gold and palladium in the first layer, denoted ε_{11}, of ~0.06 eV. The effect of the repulsion between gold and palladium is explored using Monte Carlo simulations, where it is found that ordered structures appear only for values of $\varepsilon_{11}/kT > 1.4$. The results are compared with previously published scanning tunneling microscopy images of gold/Pd(111) alloys, and the measured gold distributions yield good agreement with the results of the Monte Carlo simulations for $\varepsilon_{11}/kT \sim 0.64$. This suggests that the experimental value of ε_{11} is ~0.02 eV, in the same range, but slightly lower than predicted by density functional theory.

DOI: 10.1103/PhysRevB.77.045422 PACS number(s): 68.03.Hj, 68.35.Dv

I. INTRODUCTION

Bimetallic surfaces have physical and chemical properties that are often quite different from those of the individual components.[1–5] In particular, palladium-gold bimetallic alloys have been found to be both active and selective catalysts for a number of reactions including CO oxidation, cyclotrimerization of acetylene to benzene, vinyl acetate synthesis, selective oxidation of alcohols to aldehydes or ketones, oxidation of hydrogen to hydrogen peroxide, and hydrocarbon hydrogenation.[6–15] They are ideal systems for fundamental study since gold and palladium are completely miscible in all proportions with only a slight lattice mismatch (~4.9%).[16]

Since gold has a lower surface energy than palladium [the surface free energy of palladium is 2.05 J/m^2,[17] and that of gold is 1.63 J/m^2 (Ref. 18)], gold is expected to preferentially segregate to the surface, and this is indeed found experimentally.[19] In addition, no ordered low-energy electron diffraction (LEED) structures other than the substrate (1 $\times$1) Bragg spots have been observed for Au/Pd(111) alloys.[20] This has been taken to indicate that the gold and palladium atoms are rather randomly distributed on the surface, and relationships between the nature of various palladium ensembles on the surface and their reactivities have been proposed by assuming such a random distribution.[6–8,10] However, recent density functional theory (DFT) calculations have suggested that the interaction energies between gold and palladium ($\varepsilon_{\text{Au-Pd}}$) between gold and gold ($\varepsilon_{\text{Au-Au}}$), and between palladium and palladium ($\varepsilon_{\text{Pd-Pd}}$) in the surface layer are rather different, predicting a net repulsive energy of ~0.078 eV, implying that the surface gold and palladium atoms may not be completely randomly distributed.[21] The distribution of gold or palladium in gold-palladium alloys has been explored using scanning tunneling microscopy (STM) on electrochemically deposited alloys with palladium coverages on a (111) alloy of 0.07 and 0.15,[22] and also for gold layers evaporated onto a Pd(111) substrate and annealed above 700 K.[23] Thus, while the experimental data for this system are somewhat limited, it is instructive to theoretically explore the distribution of surface ensembles as a function of the interaction energies and to compare the results with the experimental data to establish first, whether the energies calculated by DFT reproduce the experimental distributions and second, to determine how large the interaction energy differences must be for ordered LEED patterns to appear. The problem is sufficiently complex that it cannot be solved analytically and the following work exploits Monte Carlo methods[24] to determine the interaction energies necessary to match the experimentally observed surface alloy structures. In addition, we have carried out an extensive set of DFT calculations in order to extend these to include interactions within the second layer and between the first and second layers. The DFT results are then parametrized using a model to establish the functional relationship between the interaction energies and the total energies calculated by DFT. This model yields extremely good agreement with the calculated energies and provides self-consistent values of the interaction energies between the components of the alloy. These values are compared with those derived by comparing the predictions of Monte Carlo theory with the available experimental data, where reasonably good agreement is found. This approach is applied in the following to the particular case of gold-palladium alloys, but the strategy outlined below is generally applicable to all alloy systems.

II. THEORETICAL METHODS

A. Density functional theory

First principles periodic DFT calculations were carried out using the Vienna *ab initio* simulation program (VASP).[25] The wave function was constructed from plane waves with an energy cutoff of 396 eV. Vanderbilt ultrasoft pseudopotentials[26] were used to describe the sharp features of the wave functions in the core region. The Perdew-Wang 91 (Ref. 27) form of the generalized gradient approximation

was used to model the gradient corrections to the correlation and exchange energies. The wave functions and electron density were converged to within 1×10^{-4} eV and the geometry was optimized until the force on each atom was less than 0.05 eV/Å. Using tighter convergence criteria for the forces did not lead to a change in the total energy greater than 0.01 eV. The geometries were optimized using a $3\times3\times1$ Γ-centered *k*-point mesh to sample the first Brillouin zone. The second-order Methfessel-Paxton occupation scheme[28] with smearing of 0.20 eV was used to determine the occupancy of each band. The energies of the optimized structures were then calculated using a $6\times6\times1$, Γ-centered *k*-point mesh, using the linear tetrahedron method with Blöchl corrections[29] to integrate over the first Brillouin zone. It was determined that optimizing the structure with a $6\times6\times1$ *k*-point mesh changed the energy by less than 0.01 eV compared to the preceding method.

The bulk palladium lattice constant was optimized yielding a value of 3.96 Å, close to the experimental bulk palladium lattice constant of 3.89 Å. The metal surface was modeled using a 3×3 unit cell comprised of four layers of atoms with 10 Å of vacuum, which separates the slab in the *z* direction. The top two layers were allowed to relax within the geometry optimization. The latter two were held fixed at their bulk lattice positions.

B. Models for surface structures

An "ideal" surface is initially defined as one in which there are no Au-Au interactions; the energy depends only on the gold coverage in the first and second layers and not on the specific arrangement of atoms in these two layers. The energy of this surface is given by

$$E^0 = E_{\mathrm{Pd}(111)} + n_{\mathrm{Au}^1}E_{\mathrm{Au}^1} + n_{\mathrm{Au}^2}E_{\mathrm{Au}^2}, \tag{1}$$

where $E_{\mathrm{Pd}(111)}$ is the energy of a pure Pd(111) slab. The parameters n_{Au^1} and n_{Au^2} are the number of gold atoms in the first and second layers, respectively, while E_{Au^1} and E_{Au^2} are the energies associated with replacing a palladium atom with a gold atom in the first and second layers in the limit of zero gold coverage.

It is then assumed that the energy of the ideal surface can be expressed as a sum of pairwise interactions between adjacent metal atoms. We use the notation M^i–N^j to denote an interaction between a metal atom of type *M* in the *i*th layer and one of type *N* in the *j*th layer. The total number of each type of interaction is $n_{M^i\text{–}N^j}$ and the energy associated with this interaction is $\varepsilon_{M^i\text{–}N^j}$. The total energy is then given by

$$E = \sum n_M\varepsilon_M + \sum n_{M^i\text{–}N^j}\varepsilon_{M^i\text{–}N^j}. \tag{2}$$

The first sum is over all metal atom types, and the second sum is over all types of interactions. The first sum, therefore, accounts for the reference energy of each metal atom.

To calculate the deviation in energy from that of the ideal surface, interactions between neighboring gold atoms must be taken into account. Consider two adjacent gold atoms, as shown in Fig. 1(a). The ideal representation of this surface can be taken as the superposition of the surfaces in Fig. 1(b)—the ideal energy would be the sum of the energies of these surfaces. If the total number of each type of interaction between neighboring metal atoms when going from Fig. 1(b) to Fig. 1(a) are counted, it is evident that two Pd^1-Au^1 interactions have been replaced by a Pd^1-Pd^1 and a Au^1-Au^1 interaction. Assuming that the total energy of a surface is given by the sum of these interactions, the deviation in the energy from ideality is given by

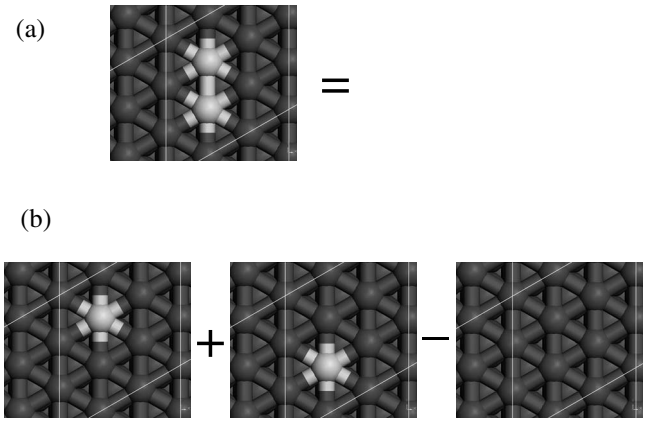

FIG. 1. Schematic depiction of the method for calculating interaction energies between atoms in the alloy film.

$$E' = \varepsilon_{11} = \varepsilon_{\mathrm{Pd}^1\text{-}\mathrm{Pd}^1} + \varepsilon_{\mathrm{Au}^1\text{-}\mathrm{Au}^1} - 2\varepsilon_{\mathrm{Pd}^1\text{-}\mathrm{Au}^1}. \tag{3}$$

If the above procedure is repeated for different surfaces with larger numbers of gold atoms in the first layer, the deviation from the ideal energy is given by $E'=n_{11}\varepsilon_{11}$ where n_{11} is the number of interactions between neighboring gold atoms in the first layer.

A similar expression holds when gold atoms are also present in the second layer. The deviation from ideality then becomes

$$E' = n_{11}\varepsilon_{11} + n_{22}\varepsilon_{22} + n_{12}\varepsilon_{12}, \tag{4a}$$

with n_{22} and n_{12} being the numbers of interactions between two gold atoms in the second layers, and between a gold atom in the first layer with one in the second layer, respectively. The energy parameters are

$$\varepsilon_{22} = \varepsilon_{\mathrm{Pd}^2\text{-}\mathrm{Pd}^2} + \varepsilon_{\mathrm{Au}^2\text{-}\mathrm{Au}^2} - 2\varepsilon_{\mathrm{Pd}^2\text{-}\mathrm{Au}^2}, \tag{4b}$$

$$\varepsilon_{12} = \varepsilon_{\mathrm{Pd}^1\text{-}\mathrm{Pd}^2} + \varepsilon_{\mathrm{Au}^1\text{-}\mathrm{Au}^2} - \varepsilon_{\mathrm{Pd}^1\text{-}\mathrm{Au}^2} - \varepsilon_{\mathrm{Pd}^2\text{-}\mathrm{Au}^1}. \tag{4c}$$

C. Monte Carlo theory

The probability *P* of an event occurring is given by the Boltzmann function and depends on the temperature *T*, and the difference in energy between the final and initial states ΔE as

$$P = \frac{1}{1+e^{\Delta E/kT}}. \tag{5}$$

From Eq. (4), the change in energy between the two states with the same number of gold atoms in each layer is given by

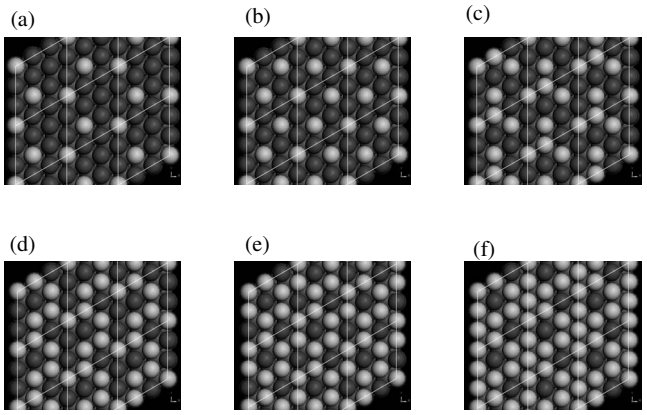

FIG. 2. Depictions of the alloy structures used for the density functional theory calculations of the energies of the various alloy surfaces, where gold is light gray and palladium dark gray.

$$\Delta E = \Delta n_{11}\varepsilon_{11} + \Delta n_{22}\varepsilon_{22} + \Delta n_{12}\varepsilon_{12}, \tag{6}$$

with Δn_{ij} being the difference in the number of Au^i-Au^j (or Pd^i-Pd^j, since the changes in these two numbers are equal for exchanges in the same layer) interactions between the final and initial states. Since the Monte Carlo calculation is carried out to examine the gold and palladium distribution in the outermost layer, then $\Delta E = \Delta n_{11}\varepsilon_{11}$, where ε_{11} is given by Eq. (3).

The Monte Carlo simulation is carried out for a particular palladium coverage Θ(Pd) by initially creating a random distribution of gold and palladium atoms on the surface. Note, however, that while this method is applied to the particular case of gold-palladium alloys, it is applicable to any alloy. A particular atom is then selected at random on the surface, and one of its nearest neighbors is then selected, also at random. If this atom type is identical to the initially chosen atom type, the exchange process is trivial, so that another atom is then randomly selected until a different atom type is encountered. The energy for the exchange of these two atoms is then calculated from Eq. (6), and the corresponding exchange probability determined from Eq. (5). The calculated probability P is then compared with a random number and if the probability P is greater than the random number, the atoms are exchanged. If it is not, the atoms are left in their initial positions. This process is repeated until no further changes in the distributions of the gold and palladium atoms are found.

This results in a calculated number of various ensembles as a function of Θ(Pd) and ε_{11}/kT. The simulation uses the Kawasaki algorithm[30] for the lattice-gas model to represent a perfectly flat (111) surface with no defects for a lattice size of 60×60 atoms with periodic boundary conditions.

III. RESULTS

A. Density functional theory

DFT calculations were carried out for a number of surface structures depicted in Fig. 2 for a 3×3 unit cell with zero to nine Au atoms in the first layer. These structures were selected as a representative set that includes all of the interactions that are fitted to the model, as described in Sec. II B.

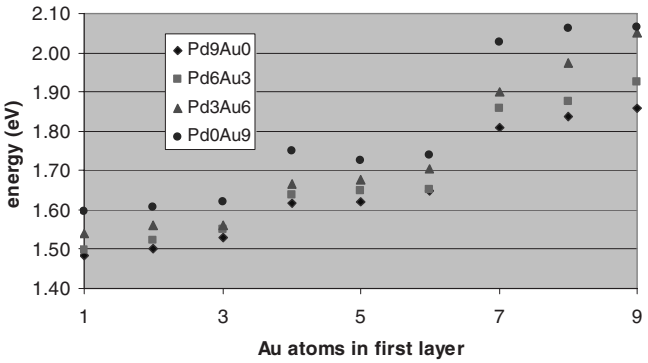

FIG. 3. Plots of the relative minimum energies for exchanging a palladium atom with a gold atom in the first layer, for different gold compositions in the first and second layers, where the different series are for different compositions in the second layer.

The second layer contained slabs with zero, three, six, and nine gold atoms. Plots of the relative minimum energies for exchanging a palladium atom with a gold atom in the first layer, for different gold compositions in the first and second layers, are displayed in Fig. 3 where the different series are for different compositions in the second layer. It becomes less favorable to replace palladium by gold as the gold content in both the first and second layers increases. The data are fitted to the model described above and the resulting comparison between the values calculated by DFT and the model are displayed in Fig. 4. The agreement between the two is excellent, and yields $\varepsilon_{11} = 0.06 \pm 0.01$ eV, $\varepsilon_{22} = 0.04 \pm 0.01$ eV, and $\varepsilon_{12} = 0.04 \pm 0.01$ eV. The excellent agreement between the energies calculated using DFT and the model described in Sec. II B that assumes only nearest-neighbor interactions indicates that this is a reasonable assumption and justifies using only nearest-neighbor interactions for the Monte Carlo simulations.

B. Monte Carlo theory

Figure 5 displays a typical distribution of ensembles obtained for an interaction $\varepsilon_{11}/kT = 1.81$. This reveals a strong variation in the number of ensembles with palladium coverage, where the number of isolated palladium atoms initially

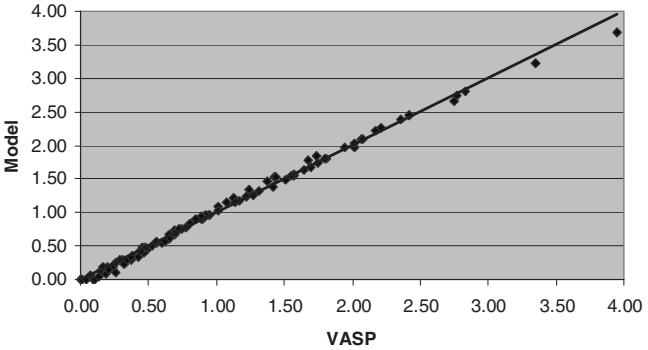

FIG. 4. Plot of the energies of the alloy calculated using the model summarized by Eq. (4) compared with the results of density functional theory.

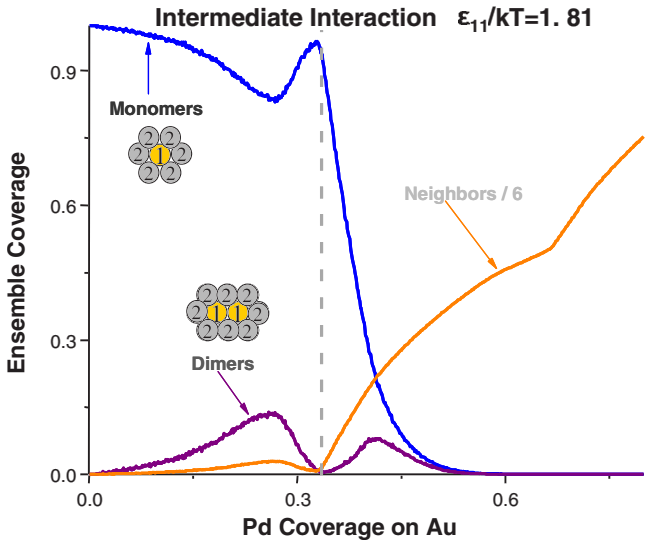

FIG. 5. (Color online) Plot of the calculated proportion of monomers and dimers for a Pd/Au(111) alloy as a function of palladium coverage for a value of $\varepsilon_{11}/kT=1.81$. Shown also plotted is the variation in the average number of nearest neighbors as a function of palladium coverage.

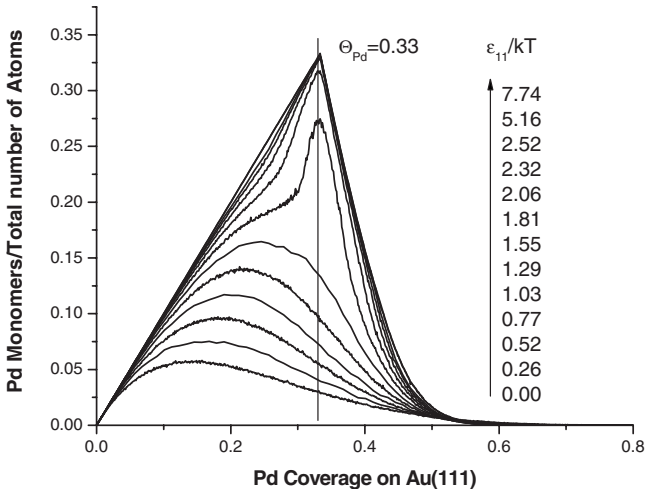

FIG. 6. Plot of the proportion of palladium monomers (the number of palladium monomers ratioed to the total number of surface atoms) as a function of palladium coverage for various values of ε_{11}/kT from a random distribution ($\varepsilon_{11}/kT=0$) to the formation of highly ordered surface ($\varepsilon_{11}/kT>1.6$).

decreases with increasing palladium coverage, and the number of adjacent palladium atoms (dimers) increases. However, as the palladium coverage approaches ~0.3 ML (monolayers), the number of dimers starts to decrease, while the number of isolated palladium atoms increases. The number of isolated atoms reaches a maximum of unity at a palladium coverage of 1/3, while the number of adjacent atoms decreases to zero. That is, the surface has ordered so that there are no adjacent palladium atoms and the alloy has formed a well-ordered $\sqrt{3}\times\sqrt{3}R30°$ superstructure. This clearly indicates that the Monte Carlo method can successfully reproduce the appearance of ordered structures. As the palladium coverage increases further, the number of isolated palladium atoms decreases rapidly since now every additional palladium atom has three nearest-neighbor palladium atoms.

In order to explore how the system evolves into ordered structures as a function of increasing values of ε_{11}/kT, Monte Carlo calculations were preformed by varying ε_{11}/kT from 0 (a completely random distribution) to ~7.74, where ordered superstructures have appeared. Figure 6 plots the fraction of the surface that forms palladium monomers where, as expected, the fraction of palladium monomers increases with increasing ε_{11}/kT because of net repulsive interactions between gold and palladium atoms. However, the peak structure at 0.33 ML, characteristic of the formation of an ordered overlayer does not appear until ε_{11}/kT has reached ~1.55. This is emphasized by the data of Fig. 7, which shows the proportion of dimers on the surface, which exhibits a drastic dip at $\Theta(\mathrm{Pd})=1/3$ for ε_{11}/kT equal to ~1.55, but which does not decrease to zero, indicating some disorder in the surface. However, for ε_{11}/kT ~1.8, the probability of there being any dimers at $\Theta(\mathrm{Pd})=1/3$ has decreased to zero, indicative of the formation of a completely ordered surface overlayer. This demonstrates clearly that, although there may be significant differences in the Au-Au, Au-Pd, and Au-Au interaction energies, ordered superstructures would not be evident until ε_{11}/kT has exceeded about 1.4.

IV. DISCUSSION

Previous DFT calculations for Au/Pd(111) alloy surfaces yielded theoretical values of $\varepsilon_{\mathrm{Pd\text{-}Pd}}=0.307$ eV, $\varepsilon_{\mathrm{Au\text{-}Au}}=0.249$ eV, and $\varepsilon_{\mathrm{Au\text{-}Pd}}=0.317$ eV in the first layer,[21] resulting in a calculated value of $\varepsilon_{11}=0.078$ eV [Eq. (3)]. Based on the results of the Monte Carlo calculations above, this implies that ordered $\sqrt{3}\times\sqrt{3}R30°$ superstructures should be observed for the Au/Pd(111) alloy at temperatures below

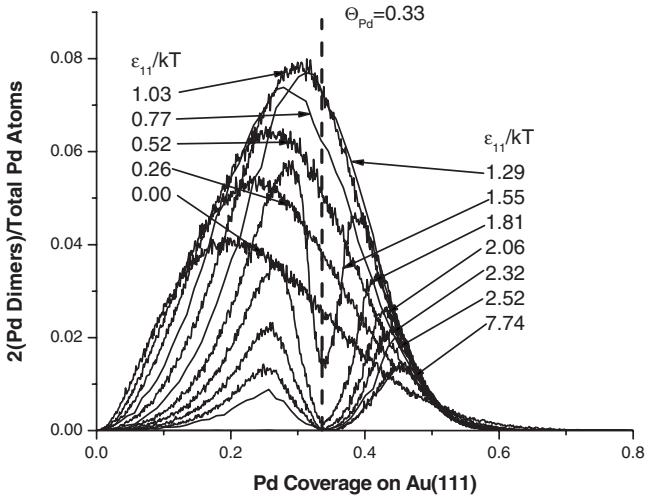

FIG. 7. Plot of the proportion of palladium atoms in dimers (twice the number of palladium dimers ratioed to the total number of surface atoms) as a function of palladium coverage for various values of ε_{11}/kT from a random distribution ($\varepsilon_{11}/kT=0$) to the formation of highly ordered surface ($\varepsilon_{11}/kT>1.6$).

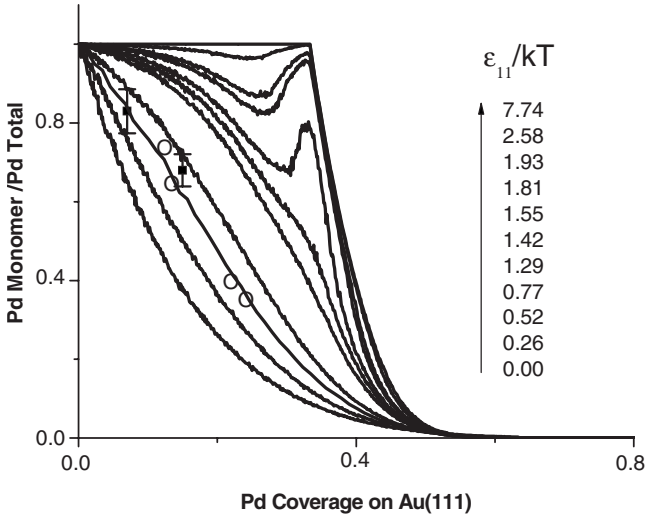

FIG. 8. Plot of the proportion of palladium monomers (the number of palladium monomers ratioed to the number of palladium surface atoms) as a function of palladium coverage for various values of ε_{11}/kT from a random distribution ($\varepsilon_{11}/kT=0$) to the formation of highly ordered surface ($\varepsilon_{11}/kT>1.6$). Shown plotted onto this curve are the results of the analysis of STM images for electrochemically deposited alloys (■) (taken from Ref. 22) and for alloys formed by depositing gold onto Pd(111) and annealing above 700 K (●) (taken from Ref. 23).

~650 K for this value of ε_{11}, while none is observed. The value of ε_{11} calculated as part of this work for exchange of atoms at the surface is somewhat lower at 0.06 ± 0.01 eV. This may arise from the slightly different conditions used for the DFT calculations in each case or from the influence of gold in the second layer that was included in this calculation, but not in previous work. This value is slightly larger than the corresponding energies for exchange between atoms in the second layer (~0.04 eV) and between the first and second layers (~0.04 eV). However, they are in reasonable agreement with previous DFT calculations [~0.08 eV (Ref. 21)] and still predict that the interaction energies are sufficiently large that ordered structures should be evident.

We can understand the origin of the peak in palladium monomer distribution at 0.33 ML by examining what happens when a pair of neighboring palladium and gold atoms is exchanged at this coverage for the perfectly ordered structure shown in Fig. 2(e). In this case, Δn_{11} is equal to 2, so $\Delta E/kT=2\varepsilon_{11}/kT$. Now consider the same exchange at lower coverages such as shown in Fig. 2(f). Here, Δn_{11} is only equal to 1 and $\Delta E/kT=\varepsilon_{11}/kT$. Thus, as the coverage of Pd approaches 0.33 ML, the energy required to deviate from the perfectly ordered configuration doubles from the value at lower coverages, resulting in increased ordering around this coverage.

Figure 8 shows a theoretical plot of the number of palladium monomer sites compared to the total amount of palladium on the surface as a function of palladium coverage, for different values of ε_{11}/kT calculated by Monte Carlo theory. Plotted also on this graph are the experimental values obtained using STM for alloy surfaces with palladium coverages of 0.07 and 0.15 for electrochemically deposited films (■),[22] as well as the results for gold evaporated onto a Pd(111) substrate heated to 700 K and above and allowed to cool to room temperature (○).[23] The data for both sets of experiments fall on the same simulation line corresponding to a value of $\varepsilon_{11}/kT=0.64\pm0.12$. This is below the critical value of ~1.4 required to form ordered alloy systems and is thus consistent with the observed lack of ordered LEED patterns for the alloy, but clearly indicates the presence of lateral interactions so that the site distribution is not random. Thus, the slightly repulsive interactions between gold and palladium result in a larger proportion of isolated palladium sites than would be expected from a completely random distribution and this effect should be taken into account when correlating reactivity with the presence of various surface ensembles. For example, the number of isolated palladium sites is approximately twice that which would have been calculated assuming that they were randomly distributed.

It is striking that the data for both electrochemically deposited and thermally annealed films lie on the same theoretical curve for $\varepsilon_{11}/kT\sim0.64$ in spite of the fact that they had completely different thermal histories. In the case of multilayers of gold evaporated onto Pd(111),[6,7] gold diffuses into the palladium substrate on heating to ~700 K to form an alloy, and the resulting distribution of gold and palladium at the surface depends on the temperature at which the mobility of gold approaches zero when the sample is subsequently cooled. Experiments carried out on films consisting of 5 ML of gold and 5 ML of palladium deposited onto a Mo(110) substrate reveal that complete intermixing occurs on annealing at approximately 600–700 K.[19] This indicates that exchange of surface and bulk gold and palladium atoms is relatively fast at ~700 K. However, the electrochemically deposited films have not been heated to such high temperatures, while the distribution of gold and palladium atoms at the surface of these alloys is identical to that formed by heating. This implies that the activation energy for the exchange of gold and palladium atoms within the first layer is sufficiently low that the gold and palladium atom distribution has attained a state close to equilibrium at 300 K (the temperature at which the STM data were collected) over the time scale required to collect the STM data. If this is the case, it is not unreasonable to choose a value of ~300 K to determine the value of ε_{11}. Taking a value of $\varepsilon_{11}/kT\sim0.64$ yields an experimental value of $\varepsilon_{11}\sim0.017$ eV. This is substantially smaller than the value predicted by DFT of ~0.06 eV (this work) or 0.08 eV.[21] They do nevertheless predict the experimentally found repulsion between gold and palladium atoms.

V. CONCLUSIONS

The present study provides a visualization of the structure of bimetallic surfaces for a wide range of interaction energies, ε_{11}. The results of density functional theory calculations for the alloys are parametrized using gold-palladium interaction energies within the first and second layers of the alloy, and between the first and second layers, and yield excellent agreement with the results of DFT calculations. The results indicate that there are net repulsive interactions between gold and palladium atoms compared to the gold-gold and

palladium-palladium interactions that are sufficiently large that the gold and palladium atoms at the surface of the alloy are not randomly distributed. The effect of these repulsive interactions is explored using Monte Carlo theory, where it is found that ordered structures do not form, even though there are repulsive interactions between gold and palladium, for values of $\varepsilon_{11}/kT < 1.4$. The results of the Monte Carlo simulations are in good agreement with experimental data for $\varepsilon_{11}/kT \sim 0.64$, consistent with the presence of repulsive interactions, but with the absence of ordered LEED patterns. Since both electrochemically deposited and thermally annealed films show identical atom distributions, this suggests that the gold and palladium atoms in the first layer are sufficiently mobile at room temperature to be close to thermal equilibrium over the time scale of a STM experiment (several hours), suggesting an experimental value of $\varepsilon_{11} \sim 0.02$ eV, slightly smaller than but within the range of that predicted by DFT.

ACKNOWLEDGMENTS

We gratefully acknowledge the support of this work by the U.S. Department of Energy, Office of Basic Energy Sciences, Division of Chemical science, under Grant No. DE-FG02-05ER15700.

*Corresponding author. FAX: (414)-229-5222; wtt@uwm.edu

[1] J. Rodriguez, Surf. Sci. Rep. **24**, 223 (1996).
[2] D. P. Woodruff, *The Chemical Physics of Solid Surfaces, Alloy Surfaces and Surface Alloys* (Elsevier, Amsterdam, 2002).
[3] M. Fernandez-Garcia, J. A. Anderson, and G. L. Haller, J. Phys. Chem. **100**, 16247 (1996).
[4] V. Ponec, Appl. Catal., A **222**, 31 (2001).
[5] T. Hager, H. Rauscher, and R. J. Behm, Surf. Sci. **558**, 181 (2004).
[6] C. J. Baddeley, M. Tikhov, C. Hardacre, J. R. Lomas, and R. M. Lambert, J. Phys. Chem. **100**, 2189 (1996).
[7] C. J. Baddeley, R. M. Ormerod, A. W. Stephenson, and R. M. Lambert, J. Phys. Chem. **99**, 5146 (1995).
[8] Y. F. Han, D. Kumar, and D. W. Goodman, J. Catal. **230**, 353 (2005).
[9] A. M. Venezia, V. La Parola, B. Pawelec, and J. L. G. Fierro, Appl. Catal., A **264**, 43 (2004).
[10] M. S. Chen, D. Kumar, C. W. Yi, and D. W. Goodman, Science **310**, 291 (2005).
[11] L. Piccolo, A. Piednoir, and J.-C. Bertolini, Surf. Sci. **592**, 169 (2005).
[12] N. Dimitratos, A. Villa, D. Wang, F. Porta, D. Su, and L. Prati, J. Catal. **244**, 113 (2006).
[13] D. I. Enache, J. K. Edwards, P. Landon, B. Solsona-Espriu, A. F. Carley, A. A. Herzing, M. Watanabe, C. J. Kiely, D. W. Knight, and G. J. Hutchings, Science **311**, 362 (2006).
[14] P. Landon, P. J. Collier, A. J. Papworth, C. J. Kiely, and G. J. Hutchings, Chem. Commun. (Cambridge) **2002**, 2058.
[15] J. K. Edwards, B. E. Solsona, P. Landon, A. F. Carley, A. Herzing, C. J. Kiely, and G. J. Hutchings, J. Catal. **236**, 69 (2005).
[16] J. Banhart, Phys. Rev. B **53**, 7128 (1996).
[17] L. Z. Mezey and J. Giber, Jpn. J. Appl. Phys. **11**, 1569 (1982).
[18] W. R. Tyson and W. A. Miller, Surf. Sci. **62**, 267 (1977).
[19] C. W. Yi, K. Luo, T. Wei, and D. W. Goodman, J. Phys. Chem. B **109**, 18535 (2005).
[20] C. J. Baddeley, C. J. Barnes, A. Wander, R. M. Ormerod, D. A. King, and R. M. Lambert, Surf. Sci. **314**, 1 (1994).
[21] D. Yuan, X. Gong, and R. Wu, Phys. Rev. B **75**, 085428 (2007).
[22] F. Maroun, F. Ozanam, O. M. Magnussen, and R. J. Behm, Science **293**, 1811 (2001).
[23] M. Ruff, Ph.D. thesis, Universität Ulm, 2000.
[24] K. Binder, *Monte Carlo Methods in Statistical Physics* (Springer-Verlag, Berlin, 1986).
[25] G. Kresse and J. Furthmüller, Phys. Rev. B **54**, 11169 (1996).
[26] D. Vanderbilt, Phys. Rev. B **41**, 7892 (1990).
[27] J. P. Perdew, J. A. Chevary, S. H. Vosko, K. A. Jackson, M. R. Pederson, D. J. Singh, and C. Fiolhais, Phys. Rev. B **46**, 6671 (1992).
[28] M. Methfessel and A. T. Paxton, Phys. Rev. B **40**, 3616 (1989).
[29] P. E. Blöchl, Phys. Rev. B **50**, 17953 (1994).
[30] K. Kawasaki, Phys. Rev. **145**, 224 (1966).